Check for updates

A facile approach to prepare porous polyamide films with enhanced electrochromic performance†

Bo-Cheng Pan,‡[a] Wei-Hao Chen,‡[a] Sheng-Huei Hsiao [ID] *[b] and Guey-Sheng Liou [ID] *[a,c]

Novel electroactive triphenylamine-based polyamide (PA) films with a purposeful porous structure have been designed and prepared by a simple route. Polymer thin films containing well dispersed electrolyte salts were prepared first, then channels of pores could be generated within the polymer film by washing the salts out. With the help of the porous channels, the diffusion rate between electroactive species and the electrolyte during the electrochemical process could be effectively increased. Consequently, the driving potential and electrochromic response time can be efficiently improved through this approach. Novel porous PA films with optimal results both in optical transparency and electrochemical properties could be readily obtained by choosing a commonly used supporting electrolyte TBABF$_4$ as a salt in this study. When the PA films containing un-washed TBABF$_4$ salt were further assembled into electrochromic devices (ECDs), the salt could then be leached out during the electrochemical redox switching process to form a porous film structure and also serves as a supporting electrolyte in ECDs simultaneously. Therefore, EC performance such as the driving potential and response time could be enhanced obviously by this simplified fabrication procedure of ECDs.

Introduction

Generally, electrochromic (EC) materials exhibit reversible changes in their optical absorption spectra during electrochemical redox procedures.[1] Due to their low power consumption, stable memory effect, and high coloration efficiency, EC materials are considered to be highly promising candidates for prospective applications, such as anti-glare car mirrors, adjustable light transmitting or light-reflective devices, sunglasses, data storage and also smart windows for buildings and public transportation.[2–5] A vast number of EC materials have been exploited for decades,[6] and some main classes include metal coordination complexes such as Prussian blue and metallo-supermolecular polymers,[7] metal oxides like tungsten trioxide (WO$_3$),[8] conjugated polymers,[9] viologens (in solution and as

adsorbed or polymeric films),[10] and arylamine-based polymers.[11] Our research group has been devoted to developing anodically EC high-performance polymers such as aromatic polyamides and polyimides.[11] When utilizing triphenylamine (TPA) derivatives as electroactive moieties within these EC polymers, they usually show high transparency in the neutral state and exhibit various colours according to their chemical structures during electrochemical oxidation. Although we have already developed abundant arylamine-based EC polymers, some crucial issues still have to be dealt with and efforts have to be made on the improvement of their EC performance, such as switching response time, coloration efficiency, EC stability, and on/off optical contrast ratio. According to previous literature, the thickness of films would dramatically influence the EC behaviour. Although the thicker films exhibited higher optical contrast, the properties of driving potential, switching time and stability would deteriorate subsequently.[12] The credible reason is the penetration difficulty of the electrolyte. The rate-determining step of the switching response is related to the counter ions going in and out through the electroactive moieties during the electrochemical redox process. For EC polymers, the kinetics of counter ion migration depends on the diffusion distance of the counter ions and the surface area of the EC materials. If porous structures could be generated in the EC polymers, there would be a substantial increase in the surface area and the creation of lots of channels throughout the whole polymer film which would lead to a

[a]*Institute of Polymer Science and Engineering, National Taiwan University, Taipei, Taiwan 10617. E-mail: gsliou@ntu.edu.tw*
[b]*Department of Chemical Engineering and Biotechnology, National Taipei University of Technology, Taipei, Taiwan 10608. E-mail: shhsiao@ntut.edu.tw*
[c]*Advanced Research Center for Green Materials Science and Technology, National Taiwan University, Taipei, Taiwan 10617*

†Electronic supplementary information (ESI) available: Experimental section, IR and NMR spectra, thermal properties, inherent viscosity, solubility and molecular weights of TPA-OMe PA, and supplementary EC behaviors, UV-Vis spectra and surface roughness of films, and ECDs derived from TPA-OMe PA films and their porous films. See DOI: 10.1039/c8nr04823a

‡ These authors contributed equally to this work.

faster diffusion rate of the counter ions. Therefore, the response time can be improved because of the easier penetration into the EC polymers during electrochemical redox reaction.

Generally, there are two main approaches to incorporate nanostructures into EC materials. First, porous EC films could be fabricated on different substrates by the hydrothermal method,[13] electrochemical deposition method,[14] *etc.* These approaches could produce various nanostructures in the EC films, such as nanorods,[15,16] nanosheets,[17] nanoflakes,[18] and porous structures.[19,20] Secondly, materials such as alumina[21] or zinc oxide[22] are firstly established as nanostructure templates, and then EC materials grow on the template. Utilization of organic materials as templates could also generate nanostructures within the EC polymers for enhancing the EC properties.[23,24] Besides, ordered nanostructured line gratings could be successfully patterned onto the electrochromic polymer through an easy and quick thermal nanoimprinting process.[25] These approaches could effectively reduce the ionic diffusion distance for electrolyte insertion and extraction. Thus, nano-architectures play a paramount role when applied to EC applications.

However, all of the above-mentioned methods require lots of efforts either on the design and synthesis of nanostructure templates or applications of special techniques and instruments. Although the EC properties could be improved by the help of these approaches, complicated fabrication processes may lead to poor feasibility in further application.

Herein, we propose a facile and simple method to obtain a porous structure within the electroactive polyamide films. We intentionally add the well compatible electrolyte salt into polymer solution before casting it to obtain a polymer hybrid film. Followed by washing out the salt from the polymer film, a porous morphology can be easily generated within the EC polyamide films. More importantly, the EC response rate of the resulting porous PA films could be expected to be effectively improved through this simple preparation process. Furthermore, we are also the first ones to introduce a nonporous structure into triphenylamine-based EC polymers for the improvement of EC properties.

Experimental section

Materials

4,4′-Diamino-4″-methoxytriphenylamine (TPA-OMe) (mp: 149–151 °C) was synthesized according to a previously reported procedure.[26] Adipoyl dichloride (TCI), copper(II) chloride (98%, SHOWA), iron(III) chloride (FeCl$_3$) (97%, SHOWA), lithium chloride (LiCl) (SHOWA), calcium chloride (CaCl$_2$) (ACROS), potassium chloride (KCl) (ACROS) and sodium chloride (NaCl) (ACROS) were used as received from commercial sources. Tetrabutylammonium perchlorate (TBAP) (ACROS) was recrystallized from ethyl acetate under a nitrogen atmosphere and then dried under vacuum. Tetrabutylammonium tetrafluoroborate (TBABF$_4$) was obtained from ion exchange of tetrabutyl-

ammonium bromide (TBABr) with sodium tetrafluoroborate (NaBF$_4$) in deionized water.

## Synthesis of triphenylamine-based electrochromic polyamide

TPA-OMe polyamide (PA) was synthesized from the diamine and adipoyl dichloride by low-temperature solution polycondensation as shown in Scheme S1.† The synthetic details, IR spectrum, NMR spectrum, inherent viscosity, molecular weight, solubility behaviour, and thermal properties of the PA are all depicted in the ESI Experimental section, Tables S1–S3, and Fig. S1–S4.† In this study, we used this TPA-OMe PA to investigate the effect of porous structures on its electrochemical and electrochromic properties.

Preparation of the porous PA films

Firstly, the salt was dissolved in *N,N*-dimethylacetamide (DMAc) and then the PA was added into the solution. We set the concentration at 4 mg per 1 mL for the preparation of PA films. And the amount of added salt was calculated as specific wt%. In order to achieve good dispersion, the solution was put into an ultrasonication instrument and then filtrated before drop-coating on the ITO-coated glass substrate. Then, 375 μL of the salt/polymer solution was dropped onto a 25 mm × 30 mm ITO-coated glass substrate. The drying process was set at 80 °C for 6 h and then 150 °C for 8 h under vacuum to obtain the films containing specific wt% of salts which were calculated precisely during preparation of the salt/polymer solution. The alpha-step profile (Fig. S5†) indicates that the quality of the coated films was good because of the small thickness deviation. The porous structure developed after immersing the salt/PA films in water and then in acetonitrile for 30 min each to wash out the salt within the film. After totally washing out the salt within the film, the porous PA film was dried at 110 °C for 4 h under vacuum. The obtained porous PA film was used for electrochemical and EC property measurements (as shown in Scheme 1).

Fabrication of ECDs

The ITO-coated glass used for ECDs was washed with water, acetone, and isopropanol for 15 min each by ultrasonication. The EC films coated onto the ITO-coated glass (25 mm × 30 mm × 1 mm, 5 Ω per square) served as the anode side. A thermosetting resin was first dispensed on another ITO glass (5 Ω per square) to trace out a 20 mm × 20 mm square frame shape by a full-auto dispenser and a tiny hole was left for the later injection of the highly transparent polymer gel electrolyte. The ECD gap was controlled by dispersing glass balls with a grain size of about 120 μm into the thermosetting resin. Covering the anode side and another ITO-coated glass with thermosetting resin together then baking them at 120 °C for 6 h. Finally, the gel electrolyte comprised of poly(methyl methacrylate) (PMMA) (M_w: 120 000), TBABF$_4$ and propylene carbonate (PC) was injected into the ECDs by the vacuum encapsulation method. PMMA (275 mg) and TBABF$_4$ (66 mg) were dissolved in PC (2 ml). The total amount of the solution inside
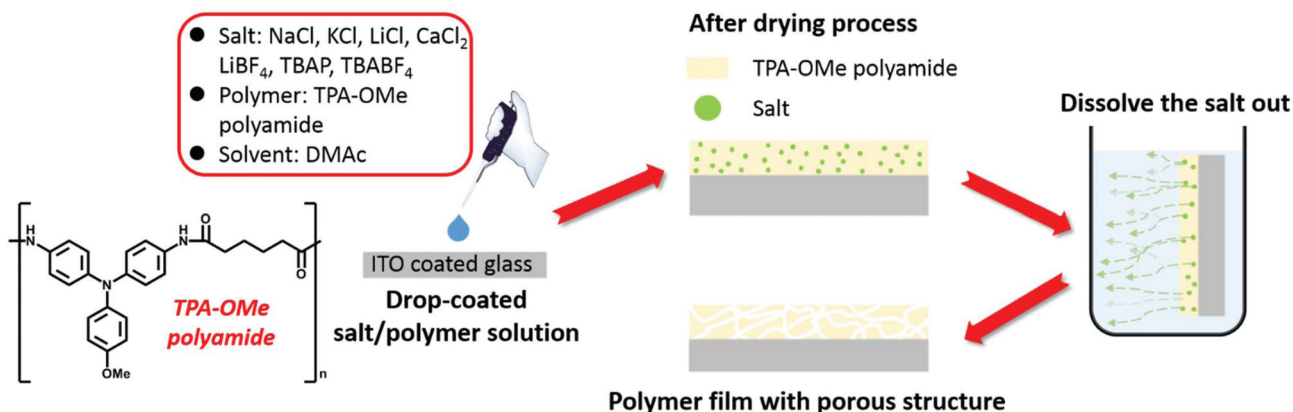
Scheme 1 Preparation procedure of porous PA films.

the ECDs after the injection was about 0.048 ml. Finally, the devices were sealed by UV-cured adhesive.

Results and discussion

Physical properties of the porous PA films

The characterization of instruments and measurement conditions are shown in the ESI.† A series of tests were designed to optimize the optical properties of the porous PA films (as shown in Tables S4–S6†). Firstly, KCl and NaCl are poorly soluble in DMAc even on heating which may lead to poor dispersion between the PA films and these salts. Consequently, non-uniform porous structures or oversized pores would be generated after washing out these salts. Secondly, the solution as well as the porous PA films exhibited a very dense yellow colour when using $CuCl_2$ and $FeCl_3$ as the salt. Thirdly, the porous PA films prepared using LiCl, $CaCl_2$, and $LiBF_4$ are easy to peel off from the ITO glass ascribed to the fact that these salts were not dispersed very well within the PA films. Because the dispersion of the salts depends on the saturated solubility and strength of interionic attraction (melting point of the salt),[27] a well dispersed system could be achieved by using salts with higher solubility. Moreover, the porous PA films prepared by using higher solubility salts could prevent the film from peeling off from the ITO glass. The porous PA films derived from 50 wt% TBAP revealed pore diameters of about 400–700 nm, but these were only 100–300 nm when using $TBABF_4$ (as shown in Fig. 1). Besides, the pore size also highly depended on their dispersion in the solvent and polymer films. As mentioned earlier, we are pursuing optimal optical properties of these porous PA films, hence $TBABF_4$ was chosen as the salt for the preparation of porous PA films used for further EC measurements.

Optical properties of the porous PA films

The diameter of pores significantly influences the surface roughness which can disturb the light path, and lead to the decrease in the optical transmittance of the porous PA films
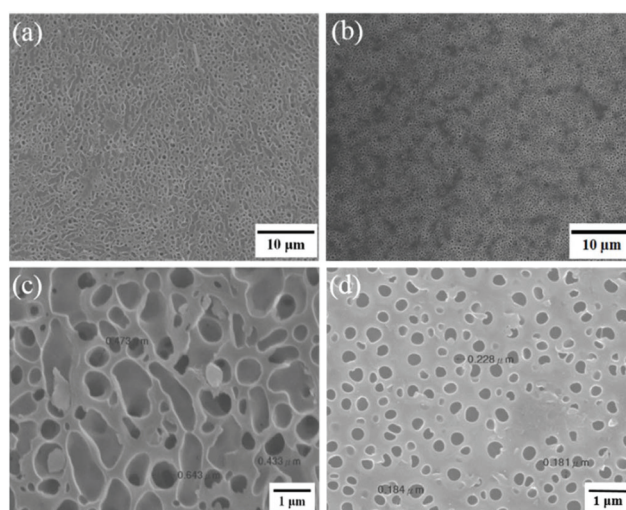

Fig. 1 SEM images of porous PA films made with (a) 50 wt% TBAP and (b) 50 wt% $TBABF_4$. (c) and (d) are the magnified images of parts of (a) and (b), respectively.

(as shown in Fig. S6 and Table S5†). Consequently, the reason why we chose the PA derived from an aliphatic diacid rather than the aromatic one is just to obtain a PA that is more colorless and has higher transmittance over the visible light region.[12] After determining which salt is appropriate for our approach, we now discuss the influence of the amount of salt content within the polymer films. PA films were prepared from the solutions with the same polymer content but different amounts of $TBABF_4$, and then were converted to porous films with different thicknesses after washing the salts out. The porous PA film made using 44 wt% of $TBABF_4$ within the film and washing the salt out exhibited the highest optical transmittance at 550 nm of about 80.4%. In contrast, the transmittance percentages of the porous PA films prepared using 62 wt% and 67 wt% $TBABF_4$ are both less than 60.0% and the films reveal a foggy surface on these porous PA films (as shown in Fig. 2, 3 and Table S6†). The huge decrease in
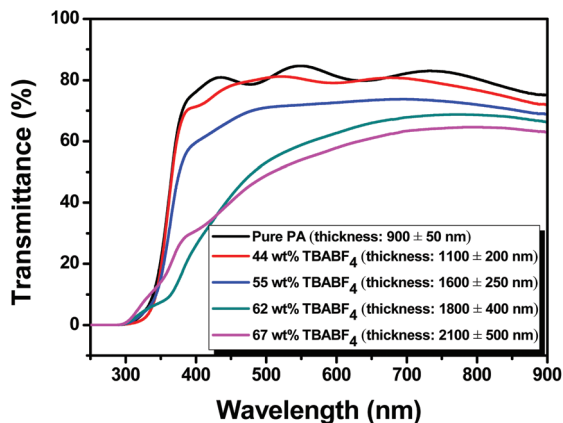
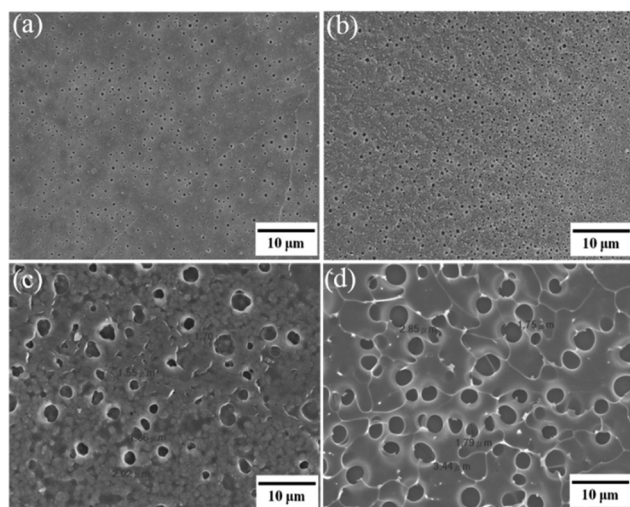**Fig. 2** UV-vis transmittance spectra of the porous PA films (relative to air as the background).

Fig. 3 SEM images of the surface of the porous PA films made with (a) 44 wt% $TBABF_4$, (b) 55 wt% $TBABF_4$, (c) 62 wt% $TBABF_4$ and (d) 67 wt% $TBABF_4$.

transmittance is caused by reflection and scattering of light which are highly dependent on the diameter of the holes and the surface roughness, and the decrease of the scattered light intensity and the increase of the transmittance are related to the film porosity just like in the Tuchikawa model.[28] Meanwhile, the pore size increased with the increase in the content of $TBABF_4$ as shown in the SEM images in Fig. 3, resulting in a lower transmittance. Therefore, the higher content of $TBABF_4$ not only enlarged the diameter of the holes but also increased the surface roughness. The AFM measurements revealed that the root mean square surface roughness (RMS) of the porous PA film containing 44 wt% $TBABF_4$ is 23.6 nm, while that of the 67 wt% $TBABF_4$ porous PA film is much larger at 357.0 nm (as shown in Fig. S6†). According to these results, the surface roughness and the diameter of the holes of the porous PA films after washing are all positively correlated to the $TBABF_4$ content. Thus, the content of $TBABF_4$

is positively correlated to the optical damage after washing it out.

Electrochemical and electrochromic properties of the porous PA films

The electrochemical behaviour of the PA films was investigated by cyclic voltammetry (CV). The PA films without and with porous structures from different salt contents were prepared for comparison. As a typical anodically EC material, the PA film without a porous structure exhibited one pair of reversible redox peaks at 1.05 V (E_{pa}) and 0.54 V (E_{pc}). The porous PA films also displayed similar reversible redox processes, while lower oxidation potentials could be detected (as shown in Fig. 4) with increasing content of $TBABF_4$. Besides, the potential difference between the pair of redox peaks ($|E_{pa} - E_{pc}|$ defined as ΔE represents the activation barrier of electron transfer[29]) became smaller which means that the rate of electron transfer became faster. Therefore, ΔE can be considered as one of the indices to confirm the electrochemical reversibility and response times. The oxidation potential and ΔE of the porous PA films made with different $TBABF_4$ contents were calculated and are summarized in Table 1. An electrochromic switching study on the porous PA films was carried out to monitor the optical contrast at their absorption maxima and
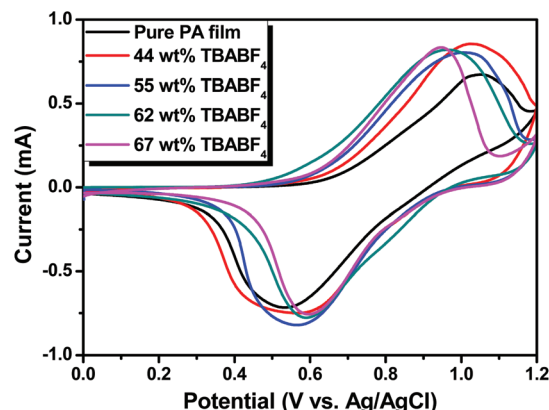

Fig. 4 Cyclic voltammetry diagrams of pure PA and porous PA films on an ITO-coated glass substrate (coated area: 25 mm × 6 mm) in electrolyte/PC solution at a scan rate of 50 mV s^{-1}.

Table 1 Oxidation potentials of the pure and porous PA films

	Oxidation potential^a (V)			
	E_{onset}	E_{pa}^{b}	E_{pc}^{c}	ΔE^d
Pure PA	0.64	1.05	0.54	0.51
With 44 wt% $TBABF_4$	0.62	1.03	0.57	0.46
With 55 wt% $TBABF_4$	0.60	1.00	0.57	0.43
With 62 wt% $TBABF_4$	0.58	0.97	0.59	0.38
With 67 wt% $TBABF_4$	0.62	0.95	0.60	0.35

^{a} Versus Ag/AgCl in PC. ^{b} E_{pa}: Anodic peak potential. ^{c} E_{pc}: Cathodic peak potential. ^{d} $\Delta E = |E_{pa} - E_{pc}|$.

to determine the switching time by stepping the potential between the neutral and oxidized states. The switching time is calculated as being the time taken to reach 90% saturation in the optical transmittance difference because it is difficult to perceive any further colour change with the naked eye after this point. As depicted in Fig. 5, the nonporous PA film revealed a 7.0 s colouring time and 6.5 s bleaching time when switching between 1.05 V and −0.1 V at 770 nm. Afterwards, the porous PA film made from the polymer solution with 44 wt% TBABF$_4$ shows a significantly improved colouring time as well as bleaching time. This can be attributed to the easier diffusion and shortened penetration distance of the counter ions during the electrochemical process with the help of these pores and channels as illustrated in Fig. 6 (cross-section images of a typical porous PA film are shown in Fig. S7†). However, the enhancement of colouring response was not so obvious with further increasing of TBABF$_4$ content, but the response rate for bleaching still enhanced with increasing content. The shortest bleaching time (3.0 s) was observed for the porous PA film made with 67 wt% TBABF$_4$. The counter ion concentration difference between the electrolyte and PA films is already quite large during the colouring process; hence the ion can easily diffuse into the film to balance the charge even without the help from the porous structure.
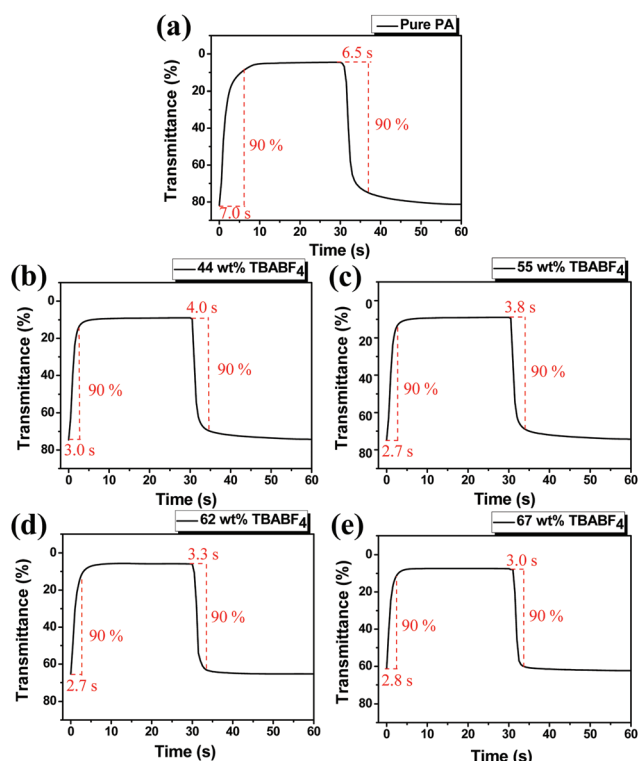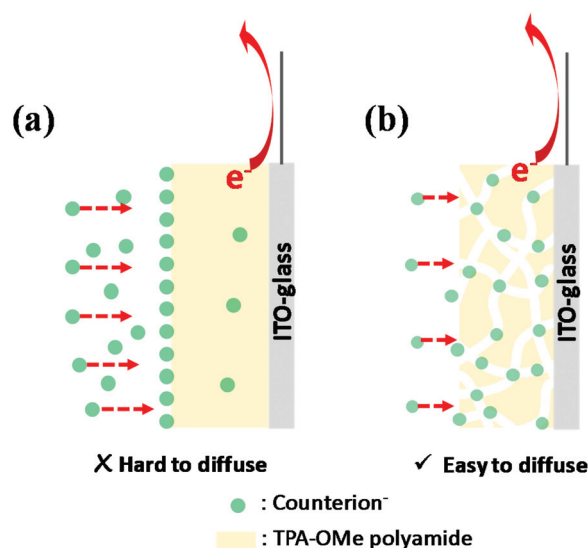

Fig. 6 Schematic diagrams of (a) the PA film without porous structures and (b) the PA film with porous structures during the electrochemical process (red arrows indicate the movement of the electrons and counter ions).

Consequently, the colouring time was significantly reduced with just a little help from the porous structure. Conversely, the concentration difference is quite small in the bleaching procedure, so it is more difficult for the ions to diffuse out from the films. Consequently, a higher porosity structure could lead to more obvious improvement in the bleaching process. However, the porous PA film made with a higher content of TBABF$_4$ resulted in a lower transmittance of the PA films. According to Fig. 2 and Table S6,† we attempted to have the T% at 550 nm of the porous PA film as high as possible which would be helpful for fabricating them into the ECDs, because the optical contrast of the ECDs during EC switching would not be enhanced if the transmittance of the porous PA film was too low at its neutral state. Therefore, we have to balance these two dilemma factors in terms of optical transmittance and response time. Thus, the porous PA films derived with less than 55 wt% TBABF$_4$ were used for the fabrication of the following ECDs.

Properties of ECDs prepared using porous PA films

According to previous results, we chose porous PA films made with 44 wt% and 55 wt% TBABF$_4$ to prepare the ECDs. The resulting porous PA films as the anode side were fabricated into the ECDs. The details of the device fabrication process are described in the Experimental section. In electrochemical tests of ECDs, the gel electrolyte solution with 0.1 M TBABF$_4$ is the minimum amount to balance the charge in the shortest time (as shown in Fig. S8†). Consequently, we set the concentration of TBABF$_4$ as 0.1 M of the injected gel electrolyte solution. Interestingly, the optical transmittance of the devices obviously increased after the electrolyte injection. Thus, the transmittance of the porous ECDs could be increased from

Fig. 5 Calculation of the colouring switching time at 770 nm for (a) 1.05 V to −0.1 V for the pure PA film without a porous structure, (b) 1.03 V to −0.1 V for the porous PA film with 44 wt% TBABF$_4$, (c) 1.0 V to −0.1 V for the porous PA film with 55 wt% TBABF$_4$, (d) 0.97 V to −0.1 V for the porous PA film with 62 wt% TBABF$_4$, and (e) 0.95 V to −0.1 V for the porous PA film with 67 wt% TBABF$_4$ (coated area: 25 mm × 6 mm).

70.5% to 75.8% (for the ECD prepared using 44 wt% TBABF$_4$ porous PA film) and from 62.8% to 67.9% (for the ECD prepared using 55 wt% TBABF$_4$ porous PA film), respectively, showing about a 5% increase at 550 nm (as shown in Fig. S9†). For porous ECDs, the injected electrolyte was used to fill the holes within the porous PA film, thus light scattering by the holes could be reduced after filling them with the electrolyte. Consequently, less light scattering occurred because of the decreasing number of open spaces and a better matching of the refractive index between the PA films and gel electrolyte solution.[30]

The electrochemical behaviour of pure and porous ECDs was investigated by CV (Fig. 7). A lower driving potential in the colouring process for the ECDs derived from the porous PA films was observed. The oxidation potential for the ECDs became lower while using the porous PA films obtained with a higher TBABF$_4$ content, from the ECD without a porous structure (2.10 V) to the 44 wt% TBABF$_4$ system (2.02 V) then the 55 wt% TBABF$_4$ system (1.95 V). Moreover, the porous structures within the ECDs could not only maintain the great optical transmittance contrast (>70%) between the neutral and coloured states but could also decrease the switching times as shown in Fig. 8, inferring that the porous systems can be applied to the ECDs and successfully improve the EC performance.

Afterward, the stability of the ECDs is determined by measuring the optical transmittance change as a function of the number of switching cycles as described in Fig. S10.† The amount of injected charge (Q_{in}) and EC coloration efficiency (η = ΔOD/Q) after several switching steps were monitored and are summarized in Tables S7 and S8.† After 30 scanning cycles, the porous ECDs exhibit less decay which can be attributed to the lower operation voltage caused by the help of the porous structure.

Fabrication of porous ECDs by *in situ* washing procedure

ECDs with porous PA films have already been confirmed to make great improvement in lowering the driving voltage and
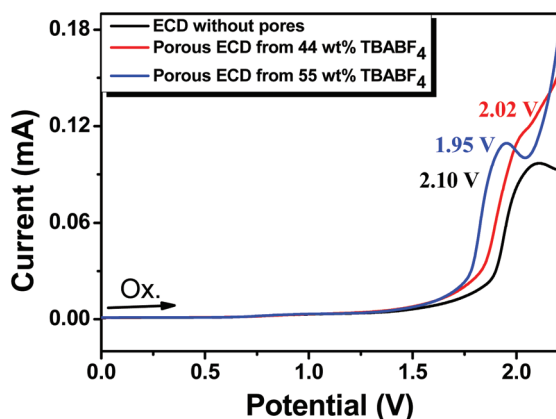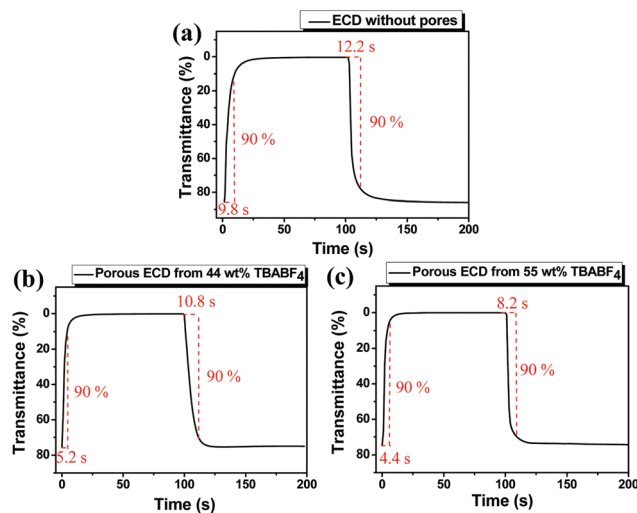
Fig. 8 Calculation of the optical switching time at 770 nm for (a) the ECD without pores at an applied potential of 2.1 V to −2.1 V, (b) the porous ECD made with 44 wt% TBABF$_4$ porous PA film at an applied potential of 2.02 V to −2.02 V, (c) the porous ECD made with 55 wt% TBABF$_4$ porous PA film at an applied potential of 1.95 V to −1.95 V with a cycle time of 200 s.

reducing the response times in the preceding section. The preparation process for the ECDs comprises preparing the porous structured films first, followed by a washing process and then fabricating them into the ECDs. However, the salts used to produce the porous structured films were wasted by the washing procedure. In this section, we therefore modify the preparation of porous ECDs without sacrificing the salts (TBABF$_4$) and also could simplify the preparation process as shown in Fig. 9 for comparison. By using the modified ECD preparation process, we first take the PA/TBABF$_4$ films without washing to assemble the ECDs, and then TBABF$_4$ could be washed out to generate the porous structure using the gel electrolyte solution in the ECDs. Thus, the salts (TBABF$_4$) used to give the porous structure still remain in the ECDs as the supporting electrolyte. It is worth noting as mentioned above that
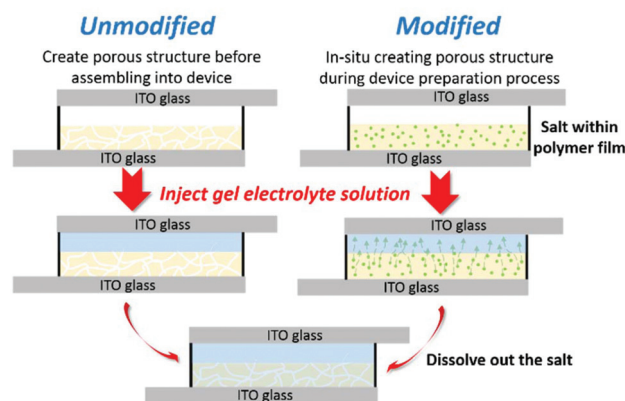
Fig. 7 Partial cyclic voltammetry diagrams of ECDs derived from pure PA and porous PA films (working area: 20 mm × 20 mm).

Fig. 9 Schematic diagram of EC device preparation processes by unmodified and modified methods, respectively.
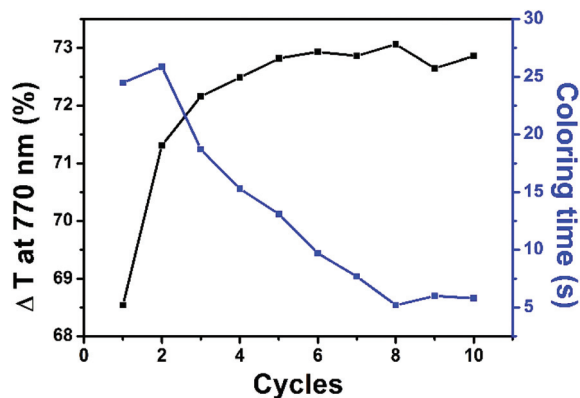
Fig. 10 The change in optical contrast at 770 nm and colouring time of porous ECDs made by the modified method (55 wt% TBABF$_4$) with applied potential cycles from 1.95 to −1.95 V.

0.1 M TBABF$_4$ in ECDs is the smallest amount to balance the charge for the shortest response time (as shown in Fig. S8†). In order to achieve 0.1 M TBABF$_4$ in the whole ECD system, the total amount of TBABF$_4$ both in the injected electrolyte solution and washing out from the blended PA hybrid films has to be precisely calculated (details are shown in Table S9†). The electrochromic properties of the porous ECDs are depicted in Fig. 10 and Fig. S11.†

The optical contrast (ΔT) at 770 nm increased gradually in the beginning 1 to 5 cycles and then levelled off to a high optical contrast (>70%). Meanwhile, the colouring time also gradually decreased from 25 s to 5 s which is similar to the porous ECDs made by the unmodified process. This delay phenomenon is a result caused by gradually drawing out the salt from the PA films for generating the porous structure and achieving 0.1 M TBABF$_4$ in the ECDs. This sensible modification of the *in situ* washing procedure can not only save the usage of salt and simplify the fabrication procedure of the ECDs but also can bring about a better EC performance compared to that achieved with the unmodified method.

Conclusions

A facile method to prepare porous PA films has been successfully developed in this study. A series of tests were designed to find out the most suitable salts used in this approach. The porous PA films prepared by washing out TBABF$_4$ exhibited the lowest optical damage of the film caused by the diameter of holes and the surface roughness. The improvements in driving voltage and response time are very significant with the help from porous structures. On the other hand, the same effects were also confirmed when these hybrid PA films were assembled directly into the ECDs without the washing process beforehand. Using this simple method, the electrochemical properties can easily be improved without any change in the material we used. Consequently, this simple preparation

method for porous PA films may be very helpful for all the film-type electrochromic devices.

Conflicts of interest

There are no conflicts to declare.

Acknowledgements

References

1 R. J. Mortimer, *Annu. Rev. Mater. Res.*, 2011, **41**, 241–268.
2 D. R. Rosseinsky and R. J. Mortimer, *Adv. Mater.*, 2001, **13**, 783–793.
3 C. G. Granqvist, *Thin Solid Films*, 2014, **564**, 1–38.
4 R. Baetens, B. P. Jelle and A. Gustavsen, *Sol. Energy Mater. Sol. Cells*, 2010, **94**, 87–105.
5 A. M. Osterholm, D. E. Shen, J. A. Kerszulis, R. H. Bulloch, M. Kuepfert, A. L. Dyer and J. R. Reynolds, *ACS Appl. Mater. Interfaces*, 2015, **7**, 1413–1421.
6 (*a*) P. M. S. Monk, R. J. Mortimer and D. R. Rosseinsky, *Electrochromism and Electrochromic Devices*, Cambridge University Press, Cambridge, UK, 2007; (*b*) *Electrochromic Materials and Devices*, ed. R. J. Mortimer, D. R. Rosseinsky and P. M. S. Monk, Wiley-VCH, Weinheim, Germany, 2015.
7 (*a*) A. Maier, A. R. Rabindranath and B. Tieke, *Chem. Mater.*, 2009, **21**, 3668–3676; (*b*) H. Higuchi, *J. Mater. Chem.*, 2014, **2**, 9331–9341.
8 D. T. Gillaspie, R. C. Tenent and A. C. Dillon, *J. Mater. Chem.*, 2010, **20**, 9585–9592.
9 (*a*) A. Patra and M. Bendikov, *J. Mater. Chem.*, 2010, **20**, 422–433; (*b*) C. M. Amb, A. L. Dyer and J. R. Reynolds, *Chem. Mater.*, 2011, **23**, 397–415; (*c*) G. Gunbas and L. Toppare, *Chem. Commun.*, 2012, **48**, 1083–1101; (*d*) P. Camurlu, *RSC Adv.*, 2014, **4**, 55832–55845.
10 (*a*) H. C. Ko, S. Kim, H. Lee and B. Moon, *Adv. Funct. Mater.*, 2005, **15**, 905–909; (*b*) G. Wang, X. Fu, J. Huang, C. Wu, L. Wu and Q. Du, *Org. Electron.*, 2011, **12**, 1216–1222.
11 (*a*) S.-H. Cheng, S.-H. Hsiao, T.-H. Su and G.-S. Liou, *Macromolecules*, 2005, **38**, 307–316; (*b*) S.-H. Hsiao, G.-S. Liou, Y.-C. Kung and H.-J. Yen, *Macromolecules*, 2008, **41**, 2800–2808; (*c*) H.-J. Yen and G.-S. Liou, *Polym. Chem.*, 2012, **3**, 255–264; (*d*) H.-J. Yen and G.-S. Liou, *Polym. Chem.*, 2018, **9**, 3001–3018.

12 H.-S. Liu, B.-C. Pan, D.-C. Huang, Y.-R. Kung, C.-M. Leu and G.-S. Liou, *NPG Asia Mater.*, 2017, **9**, e388.

13 C.-H. Lu, M. H. Hon and I.-C. Leu, *J. Electron. Mater.*, 2017, **46**, 2080–2084.

14 G. Cai, M. Cui, V. Kumar, P. Darmawan, J. Wang, X. Wang, A. L.-S. Eh, K. Qian and P. S. Lee, *Chem. Sci.*, 2016, **7**, 1373–1382.

15 J. Zhou, S. Lin, Y. Chen and A. M. Gaskov, *Appl. Surf. Sci.*, 2017, **403**, 274–281.

16 F. Zheng, W. Man, M. Guo, M. Zhang and Q. Zhen, *CrystEngComm*, 2015, **17**, 5440–5450.

17 L. Liang, J. Zhang, Y. Zhou, J. Xie, X. Zhang, M. Guan, B. Pan and Y. Xie, *Sci. Rep.*, 2013, **3**, 1936.

18 S. Poongodi, P. S. Kumar, D. Mangalaraj, N. Ponpandian, P. Meena, Y. Masuda and C. Lee, *J. Alloys Compd.*, 2017, **719**, 71–81.

19 W. L. Kwong, N. Savvides and C. C. Sorrell, *Electrochim. Acta*, 2012, **75**, 371–380.

20 C. C. Chen, *J. Nanomater.*, 2013, **2013**, 785023.

21 A. Garreau and J. L. Duvail, *Adv. Opt. Mater.*, 2014, **2**, 1122–1140.

22 X. J. Lv, J. W. Sun, B. Hu, M. Ouyang, Z. Y. Fu, P. J. Wang, G. F. Bian and C. Zhang, *Nanotechnology*, 2013, **24**, 9.

23 Y. Shi, Y. Zhang, K. Tang, Y. Song, J. Cui, X. Shu, Y. Wang, J. Liu and Y. Wu, *RSC Adv.*, 2018, **8**, 13679–13685.

24 M. Ouyang, S.-B. Huang, Y.-G. Han, X.-J. Lü, Y. Yang, Y.-Y. Dai, Y.-K. Lü and C. Zhang, *Acta Phys.-Chim. Sin.*, 2015, **31**, 476–482.

25 W. T. Neo, X. Li, S.-J. Chua, K. S. Ling Chong and J. Xu, *RSC Adv.*, 2017, **7**, 49119–49124.

26 C.-W. Chang, G.-S. Liou and S.-H. Hsiao, *J. Mater. Chem.*, 2007, **17**, 1007–1015.

27 T. Graves-Abe, F. Pschenitzka, H. Jin, B. Bollman, J. Sturm and R. Register, *J. Appl. Phys.*, 2004, **96**, 7154–7163.

28 S. Tuchikawa, *Useful and advanced information in the field of near infrared spectroscopy*, Research Signpost, Trivandrum, India, 2003, pp. 293–307.

29 R. S. Nicholson and I. Shain, *Anal. Chem.*, 1964, **36**, 706–723.

30 Z. Fang, H. Zhu, C. Preston, X. Han, S. Lee, X. Chai, G. Chen and L. Hu, *J. Mater. Chem. C*, 2013, **1**, 6191–6197.